Reaction Chemistry & Engineering

Vapor phase coupling of n-butanol over the mixed catalyst system PdZn/SiO2+TiO2

Journal:	*Reaction Chemistry & Engineering*
Manuscript ID	RE-ART-09-2024-000474.R2
Article Type:	Paper
Date Submitted by the Author:	26-Dec-2024
Complete List of Authors:	Wegener, Evan; USDA-ARS,

Vapor phase coupling of n-butanol over the mixed catalyst system $PdZn/SiO_2+TiO_2$

Evan C. Wegener*[a]

Received 00th January 20xx,
Accepted 00th January 20xx

DOI: 10.1039/x0xx00000x

Coupling fermentation derived oxygenates via Guerbet-type reactions offers a potential route for producing fuels and chemicals from agricultural feedstocks. In this work the vapor phase reactions of n-butanol over a bimetallic $PdZn/SiO_2$ catalyst and physical mixtures of $PdZn/SiO_2$ and TiO_2 were studied. The bimetallic catalyst was highly selective for n-butanol dehydrogenation without the subsequent decarbonylation of butanal which is characteristic of monometallic Pd nanoparticles. When combined with TiO_2, a known aldol condensation catalyst, the bifunctional system performs Guerbet-type coupling reactions and produces mixtures of C_8 oxygenates and higher-order products including C_7, C_8, and C_{12} hydrocarbons. Results show that within the reaction network $PdZn/SiO_2$ performs dehydrogenation/hydrogenation reactions and decarbonylates C_8 aldehydes to form C_7 hydrocarbons. TiO_2 catalyzes aldol condensation and alcohol dehydration reactions responsible for producing C_8 and C_{12} hydrocarbons. Based on the developed understanding of the function of each catalyst, it was shown that increasing the Brønsted acidity of the TiO_2 catalyst resulted in an increase in the production of C_8 hydrocarbons relative to C_{12} hydrocarbons. This work demonstrates the ability of bimetallic Pd-based catalysts that are selective for alcohol dehydrogenation to participate in Guerbet-type coupling reactions and that their combination with an appropriate aldol condensation/dehydration catalyst is an effective strategy to produce higher molecular weight oxygenates and hydrocarbons from renewable resources.

Introduction

To increase the marketability of agricultural products there is a growing desire to produce alternatives for petroleum-derived materials from renewable recourses. Short chain oxygenates (e.g., alcohols, carbonyls, carboxylic acids) produced by the fermentation of biomass are attractive feedstocks for producing fuels and chemicals due to their ability to undergo a variety of chemical transformations [1, 2]. One upgrading route that has garnered substantial attention is the coupling of alcohols to higher molecular weight products through Guerbet-type reactions [3, 4].

The conversion of ethanol to products such as n-butanol, C_{6+} alcohols, and olefins for uses including fuels, fuel precursors, and chemical building blocks has been a large focus of alcohol-coupling research [5-7]. The coupling of n-butanol, which in addition to the ethanol-based route can also be produced directly from biomass by the acetone-butanol-ethanol (ABE) fermentation [8, 9], is a reaction of interest since it can produce C_{8+} oxygenates and hydrocarbons that can serve as building blocks for a variety of chemicals and fuels. To date, the Guerbet reaction of n-butanol has primarily been carried out at high pressures in the liquid phase [10-12] with the goal of producing 2-ethylhexanol, a high production volume chemical used in the synthesis of plasticizers and other specialty chemicals [13]. However, the vapor phase Guerbet coupling of n-butanol to 2-ethylhexanol has recently been reported [14-16]

It is commonly accepted that the Guerbet-type coupling of primary alcohols proceeds through a series of reaction steps, which are shown for n-butanol in Scheme 1 [4, 17, 18]. The reaction sequence begins with the dehydrogenation of the alcohol to the corresponding aldehyde (R1) that then couples with a second carbonyl molecule via an aldol condensation step to produce an alkenal (R2). This alkenal can undergo a variety of higher order reactions including hydrogenation to an aliphatic aldehyde (R3/R3'), a second aldol condensation to higher molecule weight oxygenates (R3''), or decarbonylation to an alkene (R3'''). Like the alkenal, the aliphatic aldehyde may undergo a second coupling reaction (R4'') or decarbonylation (R4'''). Additionally, it can be reduced to an alcohol (R4/R4') that can be subsequently deoxygenated to an alkene (R5). Reduction-deoxygenation pathways analogues to the alkenal/aldehyde also exist for the C_{12} oxygenates produced from a second aldol condensation (R6/R6'). Unwanted side reactions including alcohol dehydration (R1'/R1''), aldehyde decarbonylation (R2'), and esterification via the Tishchenko reaction (R2'') may also occur and limit the yield of Guerbet coupling-derived products. Like the condensed phase studies the production of 2-ethylhexanol has been the focus of vapor phase n-butanol coupling reports. However, the C_7/C_8 hydrocarbons and C_{12} oxygenates produced via higher-order reactions could be of potential interest as precursors to fuels and other value-added chemicals. Hence, being able to direct the selectivity of alcohol coupling to a desired higher order product type would be of value.

A wide array of heterogeneous catalysts has been reported to be active for vapor phase Guerbet and aldol condensation reactions with materials such as mixed-metal oxides, [19-21] hydroxyapatites, [22-24] and titania [25-27] being extensively studied. Additionally, combining an aldol condensation catalyst with a selective alcohol dehydration catalyst, like Cu, has been shown to be a highly effective strategy to promote Guerbet-type coupling reactions.[28-30] Like Cu-based catalysts, palladium alloys have been shown to be selective for producing aldehydes from alcohols during dehydrogenation reactions. [31, 32] This contrasts monometallic palladium catalysts which are known to decompose primary alcohols through a sequential dehydrogenation/decarbonylation pathway. [33, 34] However, there are limited reports of palladium alloys being used as promoters for Guerbet-type coupling reactions in the vapor phase.

Goulas et al. reported that a Pd-Cu alloy supported on carbon with hydrotalcite was an effective catalyst for the vapor

[a] USDA, Agricultural Research Service, National Center for Agricultural Research, Renewable Product Technology, 1815 N. University St. Peoria, IL 61604 USA. E-mail: evan.wegener@usda.gov

† Electronic supplementary information (ESI) available. See DOI: 10.1039/x0xx00000x

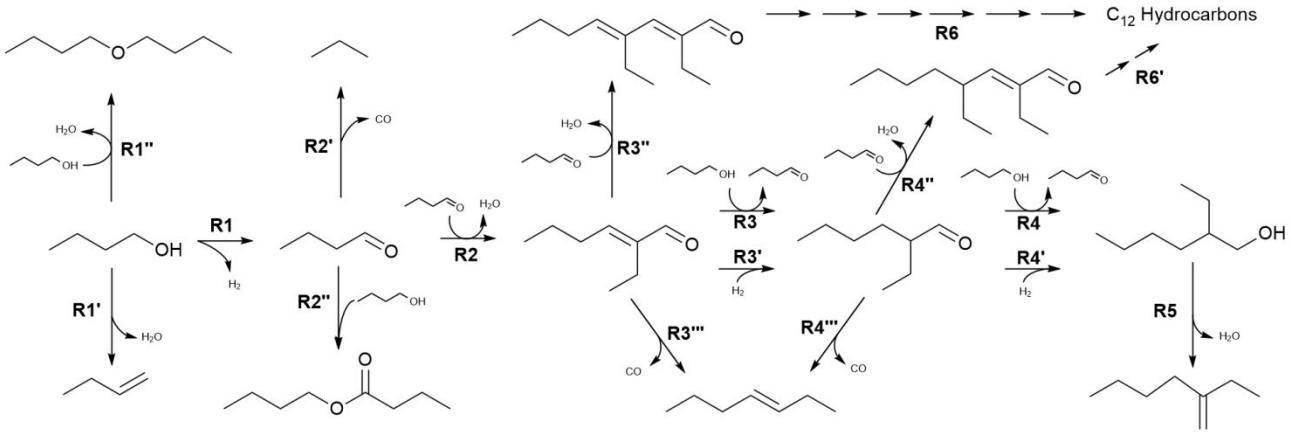

Scheme 1: Possible reaction pathways during the Guerbet-type coupling of n-butanol

phase coupling of ABE mixtures, exhibiting higher coupling production rates than a Cu-hydrotalcite material, but higher selectivity than Pd-hydrotalcite [35]. The improved performance of the alloy relative to the individual metals was credited to its high activity for alcohol dehydrogenation, like Pd, but low selectivity towards decarbonylation, like Cu. Subramaniam et al. showed the addition of Pd to a mixed ZnO-ZrO_2 catalyst increased the yields of C_{5+} ketones during ethanol coupling as compared to a Pd-free material.[36] The higher yields were attributed to the formation of a PdZn alloy, which increased ethanol dehydrogenation rates and enhanced the hydrogenation of intermediates believed to cause catalyst deactivation. The results of these studies suggest that Pd alloys that are selective for alcohol dehydrogenation can be paired with aldol condensation catalysts to make bifunctional catalyst systems effective for Guerbet-type coupling reactions in the vapor phase.

This work reports on the use of a mixed catalyst bed comprised of a silica supported Pd-Zn catalyst and P25 titania (TiO_2) to perform the vapor phase coupling of n-butanol. The bimetallic catalyst is shown to be highly selective for n-butanol dehydrogenation and, when paired with TiO_2, the mixed catalyst system produces C_8 oxygenates along with C_7, C_8, and C_{12} hydrocarbons. The effect of the TiO_2:PdZn/SiO_2 ratio in the catalyst bed and contact time on the conversion and product selectivities was studied. Additionally, based on the developed understanding of the role each catalyst plays within the reaction network the TiO_2 catalyst was modified in attempts to direct the selectivity to a specific coupling product.

Experimental

Catalyst Synthesis

The bimetallic Pd-Zn catalyst (nominal loadings: 1 wt% Pd and 3 wt% Zn) was prepared by sequential charge enhanced incipient wetness impregnation of the silica support. First, 3.06 g of $Zn(NO_3)\cdot XH_2O$ (Fischer Scientific) was dissolved in 5 mL of nano-pure water (Barnstead, 18.3 MΩ-cm) in a 25 mL volumetric flask, making a clear solution. Next, 5 mL of aqueous NH_4OH (28 wt%, Fisher Scientific) was added, which formed a white precipitate. The precipitate dissolved with the addition of water to a total volume of 25 mL yielding a clear solution with a pH =11. The solution was added to 21.75 g of the silica support (Davisil Grade 62: particle size =74-250 µm, surface area =300 m^2/g, pore volume =1.15 cm^3/g, Sigma Aldrich) dropwise with constant stirring. The impregnated catalyst was dried at room temperature in air for 24 h, and then calcined in a muffle furnace at 300 °C (3.5 ˚C/min ramp rate) for 2 h. The resultant catalyst was named Zn/SiO_2.

For the addition of Pd to Zn/SiO_2, 1.57 g of an aqueous 10 wt% $Pd(NH_3)_4(NO_3)_2$ solution (Sigma Aldrich) was weighed into a 5 mL volumetric flask and the total volume was brought up to 5 mL with 28 wt% aqueous NH_4OH yielding a solution with a pH =12. This solution was added dropwise with stirring to 4.55 g of the Zn/SiO_2 catalyst. The solid was dried at room temperature in air for 1 h, and then at 120 °C in air overnight. The dried catalyst was calcined in a muffle furnace at 200 °C (4.5 °C/min ramp rate) for 2 h. Following calcination, the catalyst was reduced in a tube furnace in flowing hydrogen (100 ccm) at 125 °C (10 °C /min ramp rate) for 30 min, and then at 450 °C (10 °C /min ramp rate) for 30 min. The final reduced bimetallic catalyst was named PdZn/SiO_2.

For comparison, a monometallic Pd catalyst (nominal loading: 1 wt% Pd) was prepared by charge enhanced incipient wetness impregnation of the silica support. 1.2 mL of aqueous 10 wt% $Pd(NH_3)_4(NO_3)_2$ was added to a 5 mL volumetric flask. To this, 0.8 mL of 28 wt% aqueous NH_4OH was added, and then the total volume was brought up to 5 mL with nano-pure water. This solution was added dropwise to 4.35 g of silica with constant stirring. The impregnated catalyst was dried at room temperature in air for 1 hr, and then at 120 °C in air overnight. The dried catalyst was calcined in a muffle furnace at 200 °C (4.5 °C /min ramp rate) for 2 h. The resultant catalyst was named Pd/SiO_2.

Titania (P25 TiO_2: nanopowder, 21 nm primary particle size) was purchased from Sigma Aldrich. To densify the catalyst the powder was mixed with equal parts water (mass basis) to form a thick paste, dried overnight at 120 °C in air, and then crushed with a mortar and pestle and sieved to a particle size of 106-300 µm. The sieved TiO_2 was then calcined in a muffle furnace at 350 °C (4.5 °C /min ramp rate) for 3 h.

Potassium modified titania (K-TiO_2) was prepared by adapting a published liquid-phase grafting procedure.[37] Syntheses were performed using multiple salts and solvents to obtain catalysts with a range of K loadings and a full list of

combinations is given in the SI. To perform the liquid-phase grafting a known amount of a K salt (K_2CO_3, KCH_3CO_2, or KOH) was dissolved in 25 mL of solvent (water or ethanol) in a 50 mL centrifuge tube. Then 2.5 g of calcined P25 TiO_2 was added to the solution and the tubes were mixed at room temperature using a Roto-Shake Genie (Scientific Industries) for 3 h. The suspensions were then centrifuged (4200 rpm, 10 min) and washed with 25 mL of the respective solvent. The resultant solids were transferred to ceramic bowls, dried at 120 °C in air overnight, and then calcined in a muffle furnace at 350 °C (4.5 °C /min ramp rate) for 3 h. The calcined catalysts were crushed with a mortar and pestle and sieved to a particle size of 106-300 µm. The K loadings for each sample was determined by X-ray fluorescence spectroscopy (Epsilon 1, PANalytical).

Tungstated titania (W-TiO_2, nominal W loading of 1.7 wt%) was synthesized using a wet impregnation method of the P25 powder. 0.46 g of H_2WO_4 (Sigma Aldrich) and 0.84 g of ammonium citrate dibasic (Sigma Aldrich) were dissolved in a mixture of 7.5 mL H_2O and 0.5 mL 28 wt% aqueous NH_4OH in a scintillation vial. 2 g of titania was added, and the slurry was mixed at room temperature using a Roto-Shake Genie (Scientific Industries) for 1.5 h. The slurry was then dried for 18 h under a flow of N_2 at 50 °C using an aluminum heating block positioned on a hot plate (Corning) with continual mixing provided by a magnetic stir bar. The resultant powder was transferred to a ceramic bowl, dried at 120 °C in air for 2 h, and then calcined in a muffle furnace at 350 °C (4.5 °C /min ramp rate) for 3 h. The resulting solid was crushed with a mortar and pestle and sieved to a particle size of 106-300 µm. The W loading was verified by X-ray fluorescence.

Catalyst characterization

X-ray diffraction (XRD) patterns were collected on a Bruker D2 Phaser using Cu Kα radiation. Patterns were collected from 5-90 2θ using a step size of 0.02 ° and count time of 0.4 s per step. Patterns were normalized to the most intense diffraction peak which corresponded to the 101 reflection of the anatase TiO_2 phase for each sample.

Physisorption data was collected using N_2 at 77 K on a Quantachrome autosorbIQ automated gas sorption analyzer. Prior to measurements samples were outgassed under dynamic vacuum at 300 °C for 4 h. Surface areas were determined using the BET method over a pressure range of $0.05 < P/P_o < 0.35$ and pore volumes and diameters were calculated from the adsorption branch using the BJH method.

Ammonia and propylamine temperature programmed desorption (TPD) experiments were performed on the same apparatus as the surface area measurements using a U-shaped flow cell. Prior to measurements, samples were treated at 300 °C in either flowing He or 10% H_2/Ar for 90 min and then cooled to 100 °C. Ammonia was adsorbed at 100 °C by flowing a mixture of 10% NH_3/N_2 over the catalyst for 30 min followed by holding the sample under a static atmosphere of the same gas for 30 min. When propylamine was used as the adsorbate the vapor was introduced by flowing He through a liquid filled bubbler at room temperature. Physisorbed species were removed by flowing He over the sample at 100 °C for 60 min. TPD measurements were performed under a flow of He using a 10 °C/min ramp rate from 100 to 700 °C. Desorbed gases were monitored using a residual gas analyzer (RGA, Pfeiffer Vacuum). Total and Brønsted acid site densities were calculated from the NH_3 signal (m/z=16) normalized by the He signal and catalyst mass. The NH_3 signal of the RGA was calibrated by decomposing different amounts of ammonium heptamolybdate tetrahydrate. Repeat TPD measurements on fresh samples were within 3% of the measured value.

Catalyst testing

Catalytic reactions were performed in the vapor phase at near atmospheric pressure (117.2-120.6 kPa) in a quartz tube reactor (I.D. 0.3 cm) in a downward flow configuration. The reactor was heated using a tube furnace (Lindberg/BlueM Mini-Mite) with a single 25.4 cm heating zone and equipped with a PID controller. Gas flows were controlled using Swagelok metering valves and were measured at the system outlet with a bubble flow meter. Liquid reactants were introduced using a syringe pump (KD Scientific, Legato 100) through a stainless-steel tube inserted into the quartz reactor positioned in the top of the heated zone where they were vaporized. A feed comprising of 10 mol% n-butanol in hydrogen (H_2) was used for dehydrogenation and coupling reactions. When 2-ethylhexanol was fed as the reactant the concentration was reduced to 5 mol% to maintain a constant molar flow rate on a carbon basis. The reactor effluent was flowed through a 4 mL glass pressure tube (Ace Glass) positioned in a water-ice bath where it was partially condensed. Non-condensed vapors and gaseous products were plumbed directly into a gas chromatograph (Agilent 8890) for online sample analysis. The outlet pressure of the system was controlled at 111.7 kPa using a back pressure regulator (Swagelok) positioned after the GC.

Catalyst particles were mixed with bare SiO_2 as a diluent and the catalyst beds were supported on a plug of quartz wool and positioned within the reactor to be centered in the heating zone. A constant bed volume was used for all reactions by adjusting the amount of SiO_2 added to PdZn/SiO_2 for n-butanol dehydrogenation and the TiO_2-PdZn/SiO_2 mixtures for coupling reactions. For n-butanol dehydrogenation reactions contact time was calculated based on the mass of PdZn/SiO_2 ($g_{PdZn/SiO2}$-min/$g_{n\text{-}Butanol}$) in the catalyst beds and values ranging from 0.2 – 6.2 min were tested. For n-butanol coupling reactions contact time was calculated based on the combined mass of TiO_2 and PdZn/SiO_2 ($g_{PdZn/SiO2+TiO2}$-min/$g_{n\text{-}Butanol}$) and values of 2.3, 4.7, and 9.4 min were tested. TiO_2:PdZn/SiO_2 mass ratios of 0.5, 1.0, and 2.0 were used for coupling reactions. Prior to starting the liquid feed, catalysts were reduced in 100 ccm of H_2 at 300 °C for 0.5 h. Once the liquid feed was started, the catalysts were allowed to stabilize for 2.0 h, after which negligible changes in the gas and liquid outlet compositions were observed.

Gas and liquid product analyses were performed by gas chromatography using a HP-5MS UI capillary column (Agilent Technologies). The outlet of the column was split and fed to a mass spectrometer (MS) for product identification, and a flame ionization detector (FID) for product quantification. Gas samples were taken every 0.25 h and liquid samples were collected every 1-1.5 h. Liquid samples were diluted with acetone and injected using a liquid auto-sampler. Reported conversions, selectivities, and yields are from samples collected from 2.0-3.5 h TOS after the catalysts had stabilized. Carbon balances were between 95 and 104% for all reactions. Conversion (X) and product selectivities (S_i) were calculated on a carbon basis using the equations:

$$X = \frac{n^0_{butanol} - n_{butanol}}{n^0_{butanol}}$$

$$S_i = \frac{n_i}{\Sigma n_i}$$

Where $n^0_{butanol}$ is the molar flow of carbon in n-butanol fed to the reactor, $n_{butanol}$ is the molar flow of carbon in n-butanol out of the reactor, and n_i is the molar flow of carbon in product i out of the reactor. Between repeat runs, conversions were within 5% of the measured value. Uncertainties in the selectivities to butanal, C_8 oxygenates, and dehydration products are 10% of the reported value while those of the higher order Guerbet products (i.e. C_7, C_8, and C_{12} hydrocarbons) and other products are 15% of the reported value.

Results and discussion

n-Butanol dehydrogenation

The β1-PdZn intermetallic phase has been shown to form in silica supported Pd-Zn catalysts synthesized using the procedure followed here.[38] This structure has also been identified in Pd and Zn containing hydrotalcite-based catalysts reported to be selective towards acetaldehyde during ethanol dehydrogenation.[31, 32] The formation of the same PdZn species suggests the PdZn/SiO_2 catalyst in this work should be selective for butanal during n-butanol dehydrogenation. To test this hypothesis, n-butanol dehydrogenation reactions were performed at 300 °C over catalyst beds containing PdZn/SiO_2 without TiO_2. Reactions at different contact times ($g_{Catalyst}$-min/$g_{n\text{-}Butanol}$) were performed to determine the effect of alcohol conversion on aldehyde selectivity and the results are shown in Figure 1.

The butanol conversion rose from 23 to 38% as the contact time was increased from 0.21 to 1.25 $g_{Catalyst}$-min/$g_{n\text{-}Butanol}$. Nearly constant conversion (average value of 42%) was seen at contact times longer than ≈2 $g_{Catalyst}$-min/$g_{n\text{-}Butanol}$. Although higher than the equilibrium conversion calculated from the data reported by Buckley and Cox (35%),[39] the invariant conversion suggests the dehydrogenation reaction reaches equilibrium over the PdZn/SiO_2 catalyst and minimal secondary reactions occur (*vide infra)*.

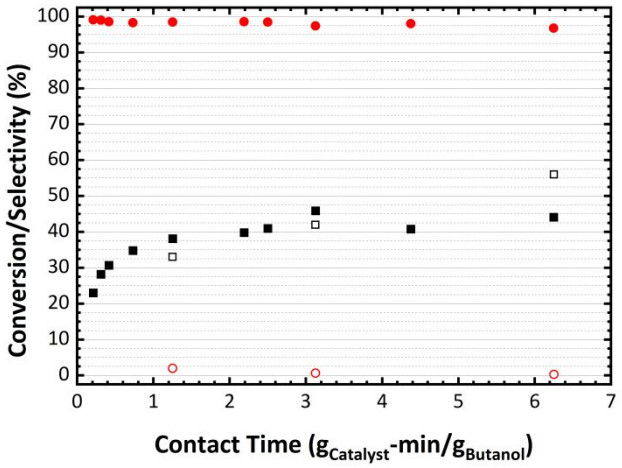

Figure 1: n-Butanol conversion (black squares) and dehydrogenation selectivity (red circles) as function of contact time. Solid shapes correspond to PdZn/SiO2 and open shapes correspond to Pd/SiO2.

Butanal was the most abundant product formed over PdZn/SiO_2 at all butanol conversions and accounted for greater than 95% of the total products. Other observed products included C_3 and C_4 hydrocarbons formed by subsequent decarbonylation of butanal and dehydration, respectively. Small amounts of aldol condensation-derived C_8 oxygenates (2-ethylhexenal, 2-ethylhexanal, and 2-ethylhexanol) were also seen. It is believed these are likely formed by residual Zn(II) on the silica surface as such species have been reported to be able to catalyze aldol condensation reactions.[40]. To account for the butanal consumed by coupling reactions, the dehydrogenation selectivity in Figure 1 was calculated as the sum of butanal and coupling-derived products divided by the total amount of products. The PdZn/SiO_2 catalyst was greater than 97% selective for dehydrogenation at all contact times tested and showed minimal selectivity towards decarbonylation. To demonstrate the marked improvement in aldehyde selectivity relative to monometallic Pd, a Zn-free material was tested for n-butanol dehydrogenation at 300 °C and contact times of 1.25, 3.13, and 6.25 $g_{Pd/SiO2}$-min/$g_{n\text{-}Butanol}$ where the PdZn/SiO_2 catalyst was approaching, or had reached, invariant conversion. At a contact time of 1.25 min the butanol conversion was 33%, slightly lower than that of PdZn/SiO_2 (38%). However, the catalyst was 98% selective towards C_3 hydrocarbons. Increasing the contact time to 3.13 and then 6.25 min gave conversions of 42 and 56%, respectively, with the latter being 14% higher than the invariant value observed at long contact times over PdZn/SiO_2. At these contact times C_3 hydrocarbons accounted for >99% of the products. The high selectivity to C_3 hydrocarbons indicates essentially all the butanal produced by dehydrogenation is rapidly decarbonylated over Pd/SiO_2.

The high selectivity for n-butanol dehydrogenation, without further decarbonylation, seen over PdZn/SiO_2 is consistent with other Pd-Zn catalyst that have been reported to be selective for ethanol dehydrogenation.[31, 32, 41, 42] Notably, under the conditions used here PdZn/SiO_2 shows negligible selectivity to esters which have been reported to form over ZnO supported Pd materials.[41] These results suggest the PdZn/SiO_2 catalyst should be able to effectively promote alcohol coupling reactions when paired with an aldol condensation catalyst by helping to facilitate alcohol dehydrogenation without producing unwanted byproducts through decarbonylation and esterification.

Butanol coupling over mixtures of TiO_2 and PdZn/SiO_2

Having confirmed PdZn/SiO_2 is capable of selectively producing butanal during n-butanol dehydrogenation, TiO_2 was added to the catalyst bed to investigate the ability of the mixture to perform alcohol coupling reactions. TiO_2 was chosen as the co-catalyst since it is a well-known aldol condensation catalyst. [25-27, 30] To verify that both catalysts are necessary for alcohol coupling to occur a series of reactions were performed using TiO_2 without PdZn/SiO_2 and liquid feeds of 100% n-butanol, 100% butanal, or a mixture of 20% of aldehyde – 80% alcohol. Feeding only n-butanol gave minimal conversion and butenes as the sole product, consistent with reports of TiO_2 being inactive for alcohol dehydrogenation. [43] As expected, the reaction of butanal over TiO_2 yielded the aldol condensation product 2-ethylhexenal (Scheme 1 – R2). When the aldehyde-alcohol mixture was fed the hydrogenated products 2-ethylhexanal and

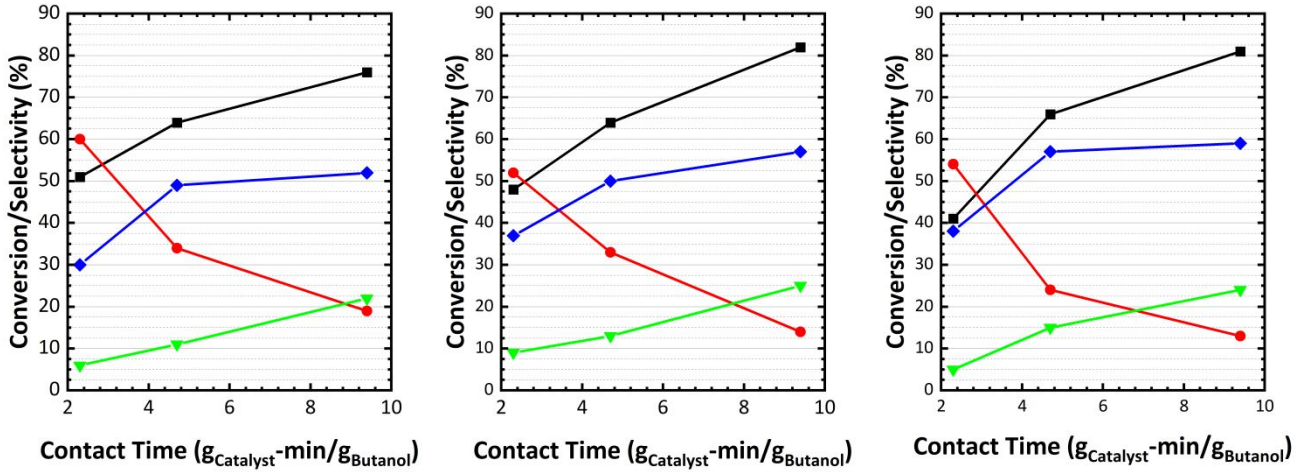

Figure 2: Conversion (black squares) and selectivity towards butanal (red circles), C_8 oxygenates (blue diamonds), and secondary Guerbet products (green triangles) as a function of contact time during n-butanol coupling reactions over mixtures of TiO_2 and $PdZn/SiO_2$. Left panel – $0.5TiO_2$:$PdZn/SiO_2$, center panel – $1.0TiO_2$:$PdZn/SiO_2$, and right panel – $2.0TiO_2$:$PdZn/SiO_2$.

2-ethylhexanol were observed in addition to 2-ethylhexenal. These are believed to be formed via reduction of 2-ethylhexenal by n-butanol (Scheme 1 – R3 and R4) as such reactions are known to occur on TiO_2 surfaces.[44] Pathways for alkenal reduction by alcohols during Guerbet-type coupling reactions over hydroxyapatites have been proposed by Bell[45] and Flaherty.[46] The route proposed by Bell involves enal hydrogenation to an enol via a Meerwein-Ponndorf-Verley (MPV) reduction, tautomerization of the enol to an aldehyde, and then a second MPV reduction to convert the aldehyde to the alcohol. Flaherty proposed that C=O and C=C hydrogenation occur through separate MPV reduction and surface-mediated H-transfer reactions, respectively. While these pathways are proposed for a different class of materials, it is likely that a MPV reduction is involved in the hydrogenation of 2-ethylhexenal on TiO_2. Although the MPV reduction does make butanal, the inability of TiO_2 to produce the aldehyde from a pure n-butanol feed indicates that the initial aldol condensation products must be derived from species formed over $PdZn/SiO_2$ and that both catalysts are required to perform alcohol coupling reactions.

Physical mixtures of the two catalysts in different mass ratios (TiO_2:$PdZn/SiO_2$ = 0.5, 1.0, and 2.0) were used to catalyze n-butanol coupling reactions at 300 °C to study how varying the relative amounts of aldol condensation and dehydrogenation catalysts affected n-butanol conversion and product selectivities. A series of reactions were performed at each mass ratio over a range of contact times where the n-butanol dehydrogenation reaction was approaching or had reached invariant conversion. Figure 2 shows the n-butanol conversions and selectivities towards butanal and aldol condensation derived products for the mixed catalyst beds (values can also be found in Table S1).

At the lowest TiO_2:$PdZn/SiO_2$ ratio (0.5) and shortest contact time tested (2.3 min) the n-butanol conversion over the mixed catalyst system was 51%, higher than the stable value seen during the dehydrogenation experiments. While butanal remained the most abundant product (60% selective) the mixed bed also made an array of products derived from aldol-condensation. C_8 oxygenates (2-ethylhexenal, 2-ethylhexanal, and 2-ethylhexanol) formed via aldol condensation of butanal (Scheme 1 – R2) and subsequent hydrogenation (Scheme 1 – R3, R3', R4, and R4') accounted for most of the coupling products with a combined selectivity of 30%. In addition to these, an array of higher order coupling products that included C_7, C_8, and C_{12} hydrocarbons (here on referred to as secondary Guerbet products) were formed and had a combined selectivity of 6%. The mass spectra of the C_7 hydrocarbons were consistent with linear heptenes formed via decarbonylation of 2-ethylhexenal (or 2-ethylhexanal with subsequent dehydrogenation) and double-bond isomerization. The C_8 hydrocarbons were identified as alkenes and alkadienes based on the molecular weights of 112 and 110 g/mol observed by GC-MS. The monoene fraction consisted of 2-ethyl-1-hexene, formed by the deoxygenation of 2-ethylhexanol, and 3-methylheptenes produced by double-bond isomerization. The best mass spectrum matches of the dienes were the di-branched compounds 2,5-dimethyl-2,4-hexadiene and 5,5-dimethyl-1,3-hexadiene. However, $PdZn/SiO_2$ catalysts have been shown to be inactive for alkane isomerization at temperatures comparable to those used here which suggests the formation of these from methylheptenes is unlikely.[47] Eagan et al. observed a single diene product during vapor phase n-butanol coupling reactions over hydroxyapatite catalysts that was tentatively identified as 3-methyl-ene-1-heptene as this would be the product formed via the Lebedev mechanism [16]. Based on these considerations, it is believed that the alkadienes observed in the current study are regioisomers of 3-methyl-ene-1-heptene formed through the Lebedev mechanism and isomerization of the double bonds. Similar to the C_8 fraction, GC-MS showed that the C_{12} compounds were comprised of alkenes (M.W. = 168 g/mol) and alkadienes (M.W. = 166 g/mol). It has been reported that aldehydes with branching at the α-carbon do not serve as nucleophiles in aldol condensation reactions, but are capable of undergoing attack by enolates [48]. The C_{12} hydrocarbons formed here are believed to arise from the addition of butanal to 2-ethylhexenal and 2-ethylhexanal (Scheme 1 – R3'' and R4'') to form the aldol products 2,4-diethyloct-2,4-dienal and 2,4-diethyloct-2-enal, which are successively hydrogenated and deoxygenated (Scheme 1 – R6 and R6'). Based on this proposed pathway and the rational for assigning the structures of the C_8 hydrocarbons, the observed C_{12} alkenes and alkadienes are believed to be regioisomers of 3-methyl-5-ethylnonene and 3

Table 1: Conversions, total coupling yields, and fractional compositions of coupling products on a carbon basis from n-butanol Guerbet reactions of mixtures of TiO2 and PdZn/SiO2

TiO_2:PdZn/SiO_2	0.5			1			2		
Contact Time (min)	2.3	4.7	9.4	2.3	4.7	9.4	2.3	4.7	9.4
Conversion (%)	51	64	76	48	64	82	41	66	81
Total Coupling Yield (%)	19	38	55	22	40	67	18	48	67
Coupling Products Composition (%)									
C_8 Oxygenates	83.3	81.3	70.6	80.9	79.6	69.4	86.0	79.1	71.1
C_7 Hydrocarbons	2.8	4.6	6.6	4.0	3.6	4.2	2.3	2.7	3.2
C_8 Hydrocarbons	9.4	9.5	12.2	11.3	9.8	13.1	7.0	9.7	12.8
C_{12} Hydrocarbons	4.5	4.6	10.6	3.7	7.0	13.3	4.7	8.5	13.0

methyl-5-ethylnonadiene. The remaining products identified at these conditions were those derived from butanol dehydration (1% selectivity) and small amounts of C_3 hydrocarbons, butyl butyrate, and 2-ethylhexyl butyrate (combined selectivity of 3% and from here on referred to as others).

Maintaining a constant TiO_2:PdZn/SiO_2 ratio of 0.5 and increasing the contact time to 4.7 min increased the n-butanol conversion to 64% and decreased the butanal selectivity to 33%. The lower butanal selectivity was accompanied by increases in the selectivities to C_8 oxygenates and secondary Guerbet products to 48 and 12%, respectively. Further increasing the contact time to 9.4 min further increased the n-butanol conversion to 64% and decreased the butanal selectivity to 19%. Only a small increase in C_8 oxygenate selectivity (52%) was seen at this longer contact time. However, the selectivity towards secondary Guerbet products nearly doubled to 23%. Across the range of contact times tested minimal change in the dehydration selectivity (2%) was observed while a small increase in the selectivity towards other products (5%) was seen.

At a contact time of 2.3 min increasing the TiO_2:PdZn/SiO_2 ratio to 1.0 resulted in a small decrease in the n-butanol conversion (48%) as compared to a mass ratio of 0.5. However, the bed was less selective for butanal (52%) and more selective for C_8 oxygenates (37%) and secondary Guerbet products (9%) than the lower TiO_2:PdZn/SiO_2 ratio. At the intermediate contact time of 4.7 min the mass ratio of 1.0 performed essentially identically to the bed with lower TiO_2 content. Increasing the contact time further to 9.4 min increased the n-butanol conversion to 82%, higher than that obtained with a mass ratio of 0.5. The higher butanol conversion was accompanied by a lower butanal selectivity (14%) and higher C8 oxygenate (57%) and secondary Guerbet product (25%) selectivities. Like the mass ratio of 0.5, minimal selectivities towards dehydration (1%) and other products (1-3%) were observed over the range of contact times.

When the TiO_2:PdZn/SiO_2 ratio was increased again to 2.0 the n-butanol conversion at a contact time of 2.3 min decreased further to 42%. Although this mixture gave a lower conversion than the other two compositions, the butanal (54%) and C_8 oxygenate (37%) selectivities were similar to those of the 1.0 mass ratio and the selectivity to secondary Guerbet products (5%) was similar to the 0.5 mass ratio. Increasing the contact time to 4.7 min resulted in a similar n-butanol conversion (66%) to the catalyst beds with less TiO_2 but gave a lower butanal selectivity (24%) and higher C_8 oxygenate (57%) and secondary Guerbet product (15%) selectivities than the other ratios. At a contact time of 9.4 min the butanol conversion and product selectivities were essentially identical to those obtained with a TiO_2:PdZn/SiO_2 ratio of 1.0. At the contact times tested minimal selectivities towards dehydration (1-2%) and other products (1-3%) were seen like the lower mass ratios.

Under the conditions tested here the mixed catalyst beds were always greater than 93% selective towards butanal and products derived from aldol condensation. At all three contact times the n-butanol dehydrogenation reaction reached equilibrium over the catalyst bed containing a TiO_2:PdZn/SiO_2 ratio of 0.5 (Table S3). With a TiO_2:PdZn/SiO_2 ratio of 1.0 n-butanol dehydrogenation did not reach equilibrium at a contact time of 2.3 min, however, the reaction was equilibrated at contact times of 4.7 and 9.4 min. Unlike the lower mass ratios, at the contact times tested the dehydrogenation reaction never reached equilibrium over the catalyst bed with a TiO_2:PdZn/SiO_2 ratio of 2.0. Although changing the relative amounts of the two catalysts resulted in differences in the equilibration of n-butanol dehydrogenation, in general, the three TiO_2:PdZn/SiO_2 mass ratios displayed similar trends in product selectivities over the range of contact times tested. Increased n-butanol conversions resulting from longer contact times led to decreased butanal selectivities as more C_8 oxygenates and secondary Guerbet products were formed. For all three mass ratios increasing the contact time from 2.3 to 4.7 minutes resulted in a larger increase in the C_8 oxygenate selectivity than that of secondary Guerbet products. However, larger increases in the selectivities of secondary Guerbet products than C_8 oxygenates were seen upon further increasing the contact time to 9.4 min.

Table 1 shows the total yield (sum of C_8 oxygenates and secondary Guerbet products) and composition of aldol-derived coupling products for the three TiO_2:PdZn/SiO_2 ratios at each contact time tested. In general, higher coupling yields were obtained at each contact time with higher TiO_2:PdZn/SiO_2 mass ratios. Although the selectivity towards C_8 oxygenates increased across the range of contact times tested they become a smaller proportion of the coupling products as they are converted into the various secondary Guerbet products. Of the conditions tested, the highest content of C_8 oxygenates (86%) was seen at a contact time of 2.3 min and TiO_2:PdZn/SiO_2 ratio of 2.0 while the highest yield of these products (58%) was achieved using

the same mass ratio and a contact time of 9.4 min. Only small differences in the composition of the secondary Guerbet products were seen between the different mass ratios. C_7 hydrocarbons typically accounted for the smallest fraction of the higher order products (2-7%) and tended to make up higher proportions at lower TiO_2:PdZn/SiO_2 ratios. At a contact time of 2.3 min C_8 hydrocarbons (8-11%) were more abundant than C_{12} hydrocarbons (3-5%), however, at a contact time of 9.4 min these species made up equivalent fractions of the higher order products.

Since the C_7/C_8 and C_{12} hydrocarbons could serve as precursors to different types of fuels (i.e. gasoline and aviation, respectively), understanding the pathways responsible for their formation is important for attempting to direct the reaction selectivity to a desired product. While the C_7 hydrocarbons are expected to form via decarbonylation of C_8 aldehydes over PdZn/SiO_2, and a second aldol condensation over TiO_2 is necessary to form C_{12} species, the deoxygenation reactions to form the C_8/C_{12} hydrocarbons could be facilitated by either catalyst. The two most likely conversion routes proceed through C_8/C_{12} alcohol intermediates and include Pd catalyzed C-O bond hydrogenolysis[49-51] and TiO_2 catalyzed dehydration.[52-55] To investigate the plausibility of these two pathways, and determine whether one route might dominate, reactions were performed with the individual catalysts and 2-ethylhexanol as reactant. For these experiments the flow rates and loading of either catalyst matched those of the 2.0TiO_2:PdZn/SiO_2 reaction with a contact time of 4.7 min. Under these conditions the conversion over PdZn/SiO_2 was 60% and 2-ethylhexanal was the major product (97%) with only small amounts of C_7 (1%) and C_8 (2%) hydrocarbons formed. The reaction of 2-ethylhexanol over TiO_2 gave a lower conversion (20%), but the only products formed were C_8 olefins. These results suggest that under the reaction conditions used here TiO_2 catalyzed dehydration of C_8 (C_{12}) alcohols is the dominant deoxygenation pathway leading to the formation of C_8 (C_{12}) hydrocarbons over the mixed beds.

From the catalytic results discussed above the roles of each catalyst within the Guerbet reaction network, and how they affect the selectivities to higher order products, can be proposed. Under the conditions used here the primary role of PdZn/SiO_2 is to perform dehydrogenation and hydrogenation reactions and this catalyst is responsible for producing the butanal that undergoes the first aldol condensations. Additionally, this catalyst is responsible for the small amounts of C_7 hydrocarbons formed as secondary Guerbet products. The initial role of TiO_2 is to perform aldol condensation reactions. Once a mixture of aldehydes and alcohols is present in the reactor the catalyst can hydrogenate aldol condensation products and generate butanal via the MPV reduction. The results also suggest alcohol dehydration over TiO_2 is chiefly responsible for the formation of C_8 and C_{12} hydrocarbons. With respect to directing the reaction selectivity towards or away from a specific secondary Guerbet product, using catalyst beds with higher TiO_2 contents limits the formation of C_7 hydrocarbons as these are formed over PdZn/SiO_2. However, preferentially making either C_8 or C_{12} hydrocarbons presents a larger challenge since TiO_2 is responsible for the formation of both species. Altering the surface chemical properties of TiO_2 to either promote or inhibit the relative preference for aldol condensation and dehydration may provide a way to direct the selectivity to a desired product.

Butanol coupling over modified TiO_2

Based on the understanding developed from n-butanol coupling over the mixed beds, the TiO_2 catalyst was modified in attempts to direct the reaction selectivity towards either C_8 or C_{12} hydrocarbons. Potassium was chosen as the modifier to decrease the C_8:C_{12} hydrocarbon ratio since small amounts on TiO_2 have been reported to preferentially poison stronger Lewis acid sites believed to be responsible for dehydration before poisoning weaker sites that catalyze aldol condensation.[53] To increase the C_8:C_{12} hydrocarbon ratio tungsten was chosen as a modifier because its addition to TiO_2 is known to generate Brønsted acid sites that are active for dehydration.[56-58]

Potassium modification of TiO_2 using a liquid-phase grafting procedure yielded catalysts with K loadings ranging from 0.14 – 10.34 wt%. The sample with a K loading of 0.61 wt%, prepared using a 0.1 M solution of K_2CO_3 in water, was selected for testing as this was close to a reported loading which led to an ≈70% reduction in the dehydration rate of isopropanol but only an ≈25% decrease in the C-C coupling rate of acetone.[53]

To verify that addition of the modifying metals only effected the surface acidic properties, and not the bulk structures of the catalysts, the parent TiO_2, K-TiO_2, and W-TiO_2 were characterized by X-ray diffraction, N_2 physisorption, and the temperature programmed desorption (TPD) of ammonia and propylamine. Figure 3 shows the X-ray diffraction patterns of the three catalysts. The pattern of TiO_2 is consistent with a mixture of anatase and rutile and is consistent with the known composition of P25. The patterns for the modified catalysts are identical to that of the parent TiO_2 indicating no changes to the bulk crystal structure occur upon addition of the modifying metal. The measured surface areas, pore volumes, and average pore diameters of the three catalysts are given in Table 2. Negligible changes in surface area and pore characteristics are seen with the addition of either K or W indicating no changes to the textural properties of TiO_2 upon modification.

Temperature programmed desorption of ammonia and propylamine were used to quantify changes in the number of total and Brønsted acid sites, respectively. Acid site densities were measured on each catalyst after treatment at 300 °C in either an inert or reducing atmosphere and the results are reported in Table 2. Following treatment in the inert atmosphere, modification with K was seen to result in large decreases in both the total (276 vs 108 μmol/g) and Brønsted

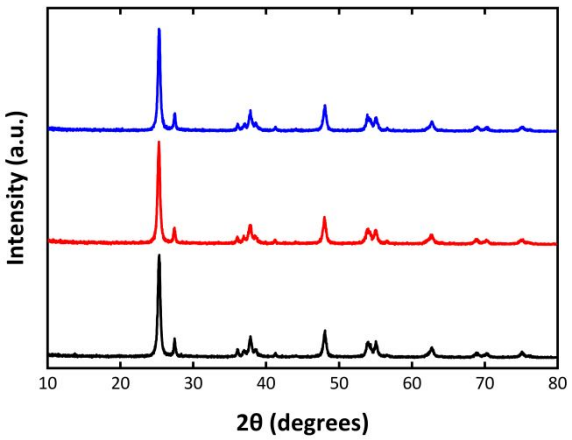

Figure 3: X-ray diffraction patterns of P25 TiO_2 (black), K-TiO_2 (red), and W-TiO_2 (blue). Patterns are offset for clarity.

Table 2: Textural properties and acid site densities of TiO_2 and the modified TiO_2 catalysts

Catalyst	BET Surface Area (m^2/g)	Pore Volume (mL/g)	Average Pore Diameter (nm)	Total Acid Sites (μmol/g)		Brønsted Acid Sites (μmol/g)	
				Inert Pretreatment	Reductive Pretreatment	Inert Pretreatment	Reductive Pretreatment
TiO_2	54	0.45	33	276	232	85	3
K-TiO_2	58	0.41	28	108	108	19	3
W-TiO_2	52	0.41	32	277	266	94	9

(85 vs 19 μmol/g) acid site densities relative to unmodified TiO_2. Pretreatment in a reducing atmosphere resulted in a decrease in the total acid site count of TiO_2 (232 μmol/g), but no change in K-TiO_2. Interestingly, the reductive pretreatment removed nearly all the Brønsted acid sites (3 μmol/g) present in these catalysts. Additionally, minimal ammonia desorption from K-TiO_2 was observed above ≈400 °C following the inert treatment and ≈430 °C for the reductive treatment as compared to ≈550 °C for TiO_2 (Figure S2). Similar changes in the desorption profile of pyridine were attributed to the preferential K coverage of stronger Lewis acid sites responsible for alcohol dehydration.[53]

Unlike K-TiO_2, W-TiO_2 treated in an inert atmosphere showed no change in the total acid site density (277 μmol/g) relative to unmodified TiO_2. However, an increase in the number of Brønsted acid sites (94 μmol/g) was observed indicative of the presence of acidic W species. Like the other two catalysts, minimal change in the total acid site density of W-TiO_2 (266 μmol/g) was seen following the reductive pretreatment. Although a large reduction in the Brønsted acid site density (9 μmol/g) was observed following the reductive pretreatment, the number of sites remained higher than the unmodified TiO_2. The combined results from the different pretreatments suggest that a fraction of the W atoms in W-TiO_2 are associated with Brønsted acidity, consistent with previous reports of similar materials having low W surface loadings.[56] Taken together, the characterization results show that modification with K and W was able to alter the surface acidic properties of TiO_2 in the desired fashions without substantially changing the bulk structural properties.

To see how the changes in surface acidity of the TiO_2 affected the relative amounts of C_8 and C_{12} hydrocarbons, n-butanol coupling reactions were performed with mixtures of PdZn/SiO_2 and the modified catalysts and the conversion, coupling yields, and coupling product compositions are shown in Table 3. Modified-TiO_2:PdZn/SiO_2 mass ratios of 2.0 were used to limit the formation of C_7 hydrocarbons. The reactions with unmodified TiO_2 at a contact time of 4.7 min were chosen as the reference cases since the different mass ratios gave nearly equivalent conversions (64-66%). Additionally, reactions of n-butanol over the modified catalysts without PdZn/SiO_2 showed no changes in the dehydrogenation activity of TiO_2 indicating the bimetallic catalyst was still necessary for generating the initial butanal for coupling.

To achieve a similar n-butanol conversion with the K-TiO_2:PdZn/SiO_2 mixture a longer contact time (9.4 min) was required. This can likely be attributed to the lower acid site density of the K modified catalyst. At a conversion of 66% the total coupling yield was 39%, lower than the TiO_2:PdZn/SiO_2 mixture with the same mass ratio, but similar to the beds with lower TiO_2 contents. Although the TPD results suggested preferential poisoning of the strong acid sites believed to catalyze dehydration, there was negligible difference in the composition of the coupling products compared to those from the unmodified TiO_2. This suggests that under the reaction conditions used here additional factors, and not solely the relative distribution of strong/weak Lewis acid sites, are important for directing the selectivity to C_{12} and away from C_8 hydrocarbons. One possible factor could be inhibition of C-C bond formation rates by co-adsorbed alcohol, as has been observed for reactions of acetaldehyde-ethanol mixtures over TiO_2.[44]

Unlike the K-TiO_2 catalyst, a similar n-butanol conversion (60%) to the beds containing unmodified TiO_2 was seen with the W-TiO_2:PdZn/SiO_2 mixture at a contact time of 4.7 min. Like the K-TiO_2 catalyst, though, the total coupling yield (36%) at this conversion was similar to the TiO_2:PdZn/SiO_2 mixtures with mass ratios of 0.5 and 1.0. Addition of W, and the generation of Brønsted acid sites, increased the fraction of C_8 hydrocarbons in the coupling product to 26.5%, compared to an average value of 9.7% seen for the unmodified TiO_2. Interestingly, the fraction of C_{12} hydrocarbons (7.0%) was essentially unchanged relative to the average value obtained over unmodified TiO_2 (6.7%), suggesting the increased C_8 fraction resulted from promoting alcohol dehydration rather than substantially decreasing the aldol condensation activity.

Table 3: Conversions, total coupling yields, and fractional compositions of coupling products on a carbon basis from n-butanol Guerbet reactions of mixtures of modified TiO_2 and PdZn/SiO_2

Catalyst	K-TiO_2	W-TiO_2
Contact Time (min)	9.4	4.7
Conversion (%)	66	60
Total Coupling Yield (%)	39	36
Coupling Product Composition (%)		
C_8 Oxygenates	81.5	65.0
C_7 Hydrocarbons	3.5	1.5
C_8 Hydrocarbons	10.0	26.5
C_{12} Hydrocarbons	5.0	7.0

Although attempts to decrease the C_8:C_{12} hydrocarbon ratio of the coupling products by reducing the acidity of TiO_2 were unsuccessful, increasing the Brønsted acidity of the catalyst did yield a higher C_8:C_{12} ratio, albeit without reducing the yield of the high molecular weight products. These results indicate that while some changes in the surface acidic properties of TiO_2 can affect the formation of certain secondary Guerbet products, they alone cannot be used to direct the selectivity of alcohol coupling reactions.

Conclusions

This work reports on the vapor phase reactions of n-butanol over a $PdZn/SiO_2$ catalyst and mixtures of the bimetallic catalyst and P25 TiO_2. The $PdZn/SiO_2$ catalyst is highly selective for n-butanol dehydrogenation to butanal without subsequent decarbonylation. Due to this, when combined with the aldol condensation catalyst TiO_2, the mixtures perform Guerbet-type coupling reactions to produce C_8 oxygenates and higher order products that include C_7, C_8, and C_{12} hydrocarbons. Within the reaction network the primary functions of $PdZn/SiO_2$ and TiO_2 are to perform dehydrogenation/hydrogenation and aldol condensation reactions, respectively. Of the secondary Guerbet products, C_7 hydrocarbons are produced over $PdZn/SiO_2$ while alcohol dehydration catalyzed by TiO_2 appears to be the dominant formation route for the C_8 and C_{12} hydrocarbons. With respect to directing selectivity to a specific coupling product, lower contact times favor C_8 oxygenates by minimizing higher order reactions and the use of catalyst mixtures with higher TiO_2:$PdZn/SiO_2$ ratios can limit the formation of C_7 hydrocarbons. Control over the relative amounts of C_8 and C_{12} hydrocarbons presents a greater challenge as the formation of both are related to the surface chemical properties of TiO_2. Although attempts to inhibit dehydration and increase the relative abundance of C_{12} hydrocarbons were unsuccessful, the addition of W to TiO_2 to promote dehydration did yield a reaction product comprising a larger fraction of C_8 hydrocarbons. Overall, this work shows when a bimetallic Pd-based catalysts that is selective for alcohol dehydrogenation is combined with an aldol condensation catalyst, the bifunctional system is highly effective for performing vapor phase Guerbet-type coupling reactions. While $PdZn/SiO_2$ and TiO_2 were the focus of this study, a variety of Pd-metal and aldol condensation catalysts may be of potential interest.

Conflicts of interest

There are no conflicts to declare.

Acknowledgements

Mention of trade names or commercial products in this publication is solely for the purpose of providing specific information and does not imply recommendation or endorsement by the U.S. Department of Agriculture. USDA is an equal opportunity provider and employer. This research was supported by the U.S. Department of Agriculture, Agricultural Research Service.

Thank you to Dr. Michael Jackson for assistance with setting up the TPD experiments and Dr. Steven Peterson for collecting X-ray diffraction patterns.

References

1. T. J. Schwartz, B. H. Shanks and J. A. Dumesic, *Current Opinion in Biotechnology*, 2016, **38**, 54-62.
2. K. A. Goulas and F. D. Toste, *Current Opinion in Biotechnology*, 2016, **38**, 47-53.
3. R. Siewert, D. H. Zaitsau, V. N. Emel'yanenko and S. P. Verevkin, *Journal of Chemical & Engineering Data*, 2019, **64**, 4904-4914.
4. D. Gabriëls, W. Y. Hernández, B. Sels, P. Van Der Voort and A. Verberckmoes, *Catalysis Science & Technology*, 2015, **5**, 3876-3902.
5. H. T. Abdulrazzaq and T. J. Schwartz, in *Ethanol*, eds. A. Basile, A. Iulianelli, F. Dalena and T. N. Veziroğlu, Elsevier, 2019, DOI: https://doi.org/10.1016/B978-0-12-811458-2.00001-8, pp. 3-24.
6. J. Sun and Y. Wang, *ACS Catalysis*, 2014, **4**, 1078-1090.
7. C. Angelici, B. M. Weckhuysen and P. C. A. Bruijnincx, *ChemSusChem*, 2013, **6**, 1595-1614.
8. E. M. Green, *Current Opinion in Biotechnology*, 2011, **22**, 337-343.
9. D. T. Jones and D. R. Woods, *Microbiological Reviews*, 1986, **50**, 484-524.
10. C. N. Neumann, S. J. Rozeveld and M. Dincă, *ACS Catalysis*, 2021, **11**, 8521-8526.
11. J. Wang, W. Yang, C. Wu, Y. Gong, J. Zhang and C. Shen, *ACS Sustainable Chemistry & Engineering*, 2020, **8**, 16960-16967.
12. R. Miller and G. Bennett, *Industrial & Engineering Chemistry*, 1961, **53**, 33-36.
13. J. I. Kroschwitz and A. Seidel, *Kirk-Othmer encyclopedia of chemical technology*, Wiley-Interscience, Hoboken, N.J., 5th edn., 2004.
14. O. V. Zikrata, O. V. Larina, K. V. Valihura, P. I. Kyriienko, D. Y. Balakin, I. Khalakhan, K. Veltruská, A. Krajnc, G. Mali, S. O. Soloviev and S. M. Orlyk, *ACS Sustainable Chemistry & Engineering*, 2021, **9**, 17289-17300.
15. O. V. Larina, K. V. Valihura, P. I. Kyriienko, N. V. Vlasenko, D. Y. Balakin, I. Khalakhan, T. Čendak, S. O. Soloviev and S. M. Orlyk, *Applied Catalysis A: General*, 2019, **588**, 117265.
16. N. M. Eagan, B. M. Moore, D. J. McClelland, A. M. Wittrig, E. Canales, M. P. Lanci and G. W. Huber, *Green Chemistry*, 2019, **21**, 3300-3318.
17. H. Aitchison, R. L. Wingad and D. F. Wass, *ACS Catalysis*, 2016, **6**, 7125-7132.
18. J. T. Kozlowski and R. J. Davis, *ACS Catalysis*, 2013, **3**, 1588-1600.
19. S. Ordóñez, E. Díaz, M. León and L. Faba, *Catal Today*, 2011, **167**, 71-76.
20. S. Abelló, F. Medina, D. Tichit, J. Pérez-Ramírez, J. C. Groen, J. E. Sueiras, P. Salagre and Y. Cesteros, *Chemistry – A European Journal*, 2005, **11**, 728-739.
21. J. I. Di Cosimo, V. K. Díez, M. Xu, E. Iglesia and C. R. Apesteguía, *Journal of Catalysis*, 1998, **178**, 499-510.
22. S. Ogo, A. Onda, Y. Iwasa, K. Hara, A. Fukuoka and K. Yanagisawa, *Journal of Catalysis*, 2012, **296**, 24-30.
23. S. Ogo, A. Onda and K. Yanagisawa, *Applied Catalysis A: General*, 2011, **402**, 188-195.

24. T. Tsuchida, J. Kubo, T. Yoshioka, S. Sakuma, T. Takeguchi and W. Ueda, *Journal of Catalysis*, 2008, **259**, 183-189.
25. F. Lin, H. Wang, Y. Zhao, J. Fu, D. Mei, N. R. Jaegers, F. Gao and Y. Wang, *JACS Au*, 2021, **1**, 41-52.
26. Z. D. Young, S. Hanspal and R. J. Davis, *ACS Catalysis*, 2016, **6**, 3193-3202.
27. S. Luo and J. L. Falconer, *Journal of Catalysis*, 1999, **185**, 393-407.
28. S. Wang and E. Iglesia, *The Journal of Physical Chemistry C*, 2016, **120**, 21589-21616.
29. T. Moteki, A. T. Rowley and D. W. Flaherty, *ACS Catalysis*, 2016, **6**, 7278-7282.
30. S. Wang, K. Goulas and E. Iglesia, *Journal of Catalysis*, 2016, **340**, 302-320.
31. J. De Waele, V. V. Galvita, H. Poelman, C. Detavernier and J. W. Thybaut, *Applied Catalysis A: General*, 2018, **555**, 12-19.
32. J. De Waele, V. V. Galvita, H. Poelman, C. Detavernier and J. W. Thybaut, *Catalysis Science & Technology*, 2017, **7**, 3715-3727.
33. J. M. Davidson, McGregor and L. K. Doraiswamy, *Industrial & Engineering Chemistry Research*, 2001, **40**, 101-107.
34. J. M. Davidson, McGregor and L. K. Doraiswamy, *Industrial & Engineering Chemistry Research*, 2001, **40**, 108-113.
35. K. A. Goulas, S. Sreekumar, Y. Song, P. Kharidehal, G. Gunbas, P. J. Dietrich, G. R. Johnson, Y. C. Wang, A. M. Grippo, L. C. Grabow, A. A. Gokhale and F. D. Toste, *Journal of the American Chemical Society*, 2016, **138**, 6805-6812.
36. S. Subramaniam, M. F. Guo, T. Bathena, M. Gray, X. Zhang, A. Martinez, L. Kovarik, K. A. Goulas and K. K. Ramasamy, *Angewandte Chemie International Edition*, 2020, **59**, 14550-14557.
37. T. C. Keller, K. Desai, S. Mitchell and J. Pérez-Ramírez, *ACS Catalysis*, 2015, **5**, 5388-5396.
38. S. C. Purdy, R. R. Seemakurthi, Garrett M. Mitchell, M. Davidson, B. A. Lauderback, S. Deshpande, Z. Wu, E. C. Wegener, J. Greeley and J. T. Miller, *Chemical Science*, 2020, **11**, 5066-5081.
39. E. Buckley and J. D. Cox, *T Faraday Soc*, 1967, **63**, 895-901.
40. W. Dai, S. Zhang, Z. Yu, T. Yan, G. Wu, N. Guan and L. Li, *ACS Catalysis*, 2017, **7**, 3703-3706.
41. M. Ouyang, S. Cao, S. Yang, M. Li and M. Flytzani-Stephanopoulos, *Industrial & Engineering Chemistry Research*, 2020, **59**, 2648-2656.
42. N. Iwasa, O. Yamamoto, R. Tamura, M. Nishikubo and N. Takezawa, *Catalysis Letters*, 1999, **62**, 179-184.
43. H. Bahruji, M. Bowker, C. Brookes, P. R. Davies and I. Wawata, *Applied Catalysis A: General*, 2013, **454**, 66-73.
44. H. Zhang, M. Y. S. Ibrahim and D. W. Flaherty, *Journal of Catalysis*, 2018, **361**, 290-302.
45. C. R. Ho, S. Shylesh and A. T. Bell, *ACS Catalysis*, 2016, **6**, 939-948.
46. T. Moteki and D. W. Flaherty, *ACS Catalysis*, 2016, **6**, 4170-4183.
47. D. J. Childers, N. M. Schweitzer, S. M. K. Shahari, R. M. Rioux, J. T. Miller and R. J. Meyer, *Journal of Catalysis*, 2014, **318**, 75-84.
48. C. A. Hamilton, S. D. Jackson and G. J. Kelly, *Applied Catalysis A: General*, 2004, **263**, 63-70.
49. A. Saraeian, G. Gupta, R. Johnson, R. W. Dorn, A. M. Kauffmann, H. Bateni, J.-P. Tessonnier, L. T. Roling, A. J. Rossini and B. H. Shanks, *ACS Sustainable Chemistry & Engineering*, 2022, **10**, 7759-7771.
50. N. Pino, S. Sitthisa, Q. Tan, T. Souza, D. López and D. E. Resasco, *Journal of Catalysis*, 2017, **350**, 30-40.
51. C. González, P. Marín, F. V. Díez and S. Ordóñez, *Industrial & Engineering Chemistry Research*, 2016, **55**, 2319-2327.
52. A. R. Riscoe, J. Oh and M. Cargnello, *Nanoscale*, 2022, **14**, 2848-2858.
53. F. Lin, Y. Lu, K. A. Unocic, S. E. Habas, M. B. Griffin, J. A. Schaidle, H. M. Meyer, III, Y. Wang and H. Wang, *ACS Catalysis*, 2022, **12**, 465-480.
54. F. Lin, Y. Chen, L. Zhang, D. Mei, L. Kovarik, B. Sudduth, H. Wang, F. Gao and Y. Wang, *ACS Catalysis*, 2020, **10**, 4268-4279.
55. P. Kostestkyy, J. Yu, R. J. Gorte and G. Mpourmpakis, *Catalysis Science & Technology*, 2014, **4**, 3861-3869.
56. T. Onfroy, G. Clet, S. B. Bukallah, T. Visser and M. Houalla, *Applied Catalysis A: General*, 2006, **298**, 80-87.
57. V. Lebarbier, G. Clet and M. Houalla, *The Journal of Physical Chemistry B*, 2006, **110**, 22608-22617.
58. J. R. Sohn and J. H. Bae, *Korean Journal of Chemical Engineering*, 2000, **17**, 86-92.

Data Availability Statement

The data supporting this article are included within the manuscript and electronic supplementary information.